

Preparation and Microstructural, Structural, Optical and Electro-Optical Properties of La Doped PMN-PT Transparent Ceramics

Fernando Andrés Londono Badillo, Jose Antonio Eiras, Flavio Paulo Milton, Ducinei Garcia

Ferroelectric Ceramics Group, Physics Department, Federal University of São Carlos, São Carlos, Brazil

Email: flondono@df.ufscar.br

Received June 30, 2012; revised July 27, 2012; accepted August 10, 2012

ABSTRACT

Transparent relaxor ferroelectric ceramics of the system lanthanum modified lead magnesium niobate have been investigated for a variety of electro-optic properties that could make these materials alternatives to $(\text{Pb},\text{La})(\text{Zr},\text{Ti})\text{O}_3$. However, a study that relates the to properties in function stoichiometric formula, has not been analyzed heretofore. Therefore, in this work the effect of A-site substitution of La^{3+} in the characterization microstructural, structural, optical and electro-optical on $(1-x)\left[\text{Pb}_{(1-3/2y)}\text{La}_y(\text{Mg}_{1/3}\text{Nb}_{2/3})\text{O}_3\right]-x\text{PbTiO}_3$ and $(1-z)\left[(1-x)\text{Pb}(\text{Mg}_{1/3}\text{Nb}_{2/3})\text{O}_3+x\text{PbTiO}_3\right]+z\text{La}_2\text{O}_3$ has been performed. It was observed that the properties according to the stoichiometric formula and the PT had a maximum whose behavior was related to the addition of lanthanum in each stoichiometries.

Keywords: Ferroelectric; Optics; Transmittance; Electro-Optical

1. Introduction

Lead magnesium niobate $\text{Pb}(\text{Mg}_{1/3}\text{Nb}_{2/3})\text{O}_3$ (PMN), as one of the most widely investigated relaxor ferroelectric with a perovskites structure, was first synthesized in the late 1950s [1]. Initially, PMN was prepared by the conventional mixed oxide method, where pyrochlore phase was inevitably produced. In order to synthesize stoichiometric perovskite PMN ceramics, Swartz and Shrout [2] proposed a columbite precursor method, where the intermediate reaction of the formation of pyrochlore phase was bypassed, which results in the stabilization of perovskites structure as compared to the mixed oxide method. Recently, a novel methodology was devised to stabilize perovskites structure by adding stable normal PbTiO_3 (PT). The formation of the solid solution increases the tolerance factor and electronegativity difference, leading to the stabilization of the perovskites structure and the enhancement of dielectric property of the relaxor ferroelectric [3].

A study of the optical, electrical and electro-optical properties of PMN-PT ceramics in function of the stoichiometrie is of interest both for possible insight into the physical nature of relaxor ferroelectrics as well as for making practical extension of its several present applications to include usage in electro-optical devices. Present applications take advantages of PMN-PT singularly ex-

cellent dielectric, low thermal expansion, and high electrostrictive properties [4]. From the viewpoint of crystal chemistry, the substitution of Ti^{4+} ions for the complex $(\text{Mg}_{1/3}\text{Nb}_{2/3})^{4+}$ ions on the B-site of the perovskite structure in the $(1-x)\text{Pb}(\text{Mg}_{1/3}\text{Nb}_{2/3})\text{O}_3-x\text{PbTiO}_3$ (PMN-PT) system leads to the outstanding properties of the PMN-PT ceramics that exhibit excellent electrical and electro-optical performance, which make them promising applications in multilayer capacitors, piezoelectric transducers and actuators and optical devices [5,6]. However, perovskite structure are extremely difficult to fabricate reproducibly without the appearance of stable pyrochlore phase, which always exist in the PMN-PT ceramics and significantly deteriorates such properties as the dielectric property [7].

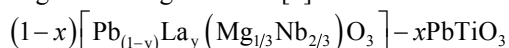
The optical transmittance as function of wavelength was studied in $\text{Pb}(\text{Mg}_{1/3}\text{Nb}_{2/3})_{0.62}\text{Ti}_{0.38}\text{O}_3$ single crystal by Wan *et al.* It was found that the crystal is transparent in the visible region and rolls off in near 450 nm. Using the Senarmont compensador method, the effective electro-optic coefficient $r_c = 42.8$ pm/V was also obtained [8]. Some effect and applications, such as photorefractive, Second-Harmonic Generation (SHG), electro-optic and elasto-optical devices, are based on the large optical property coefficient of the materials [9,10]. The knowledge of factors that can modify these properties is desirable to find new application of the relaxor and elec-

tro-optical materials. In this work, ceramics in the PMN-PT system were prepared by doping with lanthanum. La addition to PMN-PT has been shown to promote densification and through hot uniaxial pressing, optically transparent materials have been achieved, allowing the determination of various optic and electro optic properties [11,12].

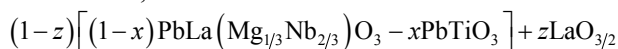
It is the purpose of this article, to report the microstructural, structural, electrical, optical and electro-optical properties according to the stoichiometric formula of lanthanum doped PLMN-XPT and PMN-XPT:La with $0.11 \leq x \leq 0.15$.

2. Experimental Procedure

The powder was synthesized by the columbite or two-stage calcining method [2]. The batch formulae were



PLMN-XPT, and



PMN-XPT:La, with $y = 0.01$, $z = 0.01$, $X = 100x$ and $0.11 \leq x \leq 0.15$. The starting materials were lanthanum oxide, La_2O_3 (Aldrich, >99% purity), niobium oxide, Nb_2O_5 (Alfa Aesar 99.9% purity), magnesium carbonate hydroxide pentahydrate, $(\text{MgCO}_3)_4 \cdot \text{Mg}(\text{OH})_2 \cdot 5\text{H}_2\text{O}$ (Aldrich 99% purity), lead oxide, PbO (MGK 99%) and titanium oxide, TiO_2 (Alfa Aesar, 99.8% purity) powders. The $(\text{MgCO}_3)_4 \cdot \text{Mg}(\text{OH})_2 \cdot 5\text{H}_2\text{O}$ was carried up to 1100°C , for 4 h, to drive off CO_2 and H_2O and obtain the correct amount of MgO for a stoichiometric reaction with Nb_2O_5 . In the first stage, MgO and Nb_2O_5 powders were ball-milled and prereacted at 1100°C for 4 h, in air, to form the columbite phase (MgNb_2O_6). In the second stage, the synthesized MgNb_2O_6 (MN) was ball-milled in isopropanol, for 24 h, with appropriate amounts of PbO , TiO_2 and La_2O_3 and heated at 900°C , for 4 h, in oxygen atmosphere, at a controlled pressure of 200 kPa. The calcined powders were pressed into pellets 10 mm in diameter and 10 mm in thickness with the addition of an appropriate amount of polyvinyl alcohol (PVA) binder. The pellets were sintered in hot uniaxial pressing in O_2 atmosphere followed for 4 h at 1220°C , and 6 MPa.

The phases and the structural parameters were determined by X-ray diffraction (XRD) using a Rigaku diffractometer, with $\text{CuK}\alpha$ radiation. The lattice parameters were calculated by least squares from the positions of the diffraction peaks. Apparent densities were determined by the Archimedes method. The microstructural features of the samples were investigated by scanning electron microscopy (SEM), using a Jeol JSM 5800 LV. The grain sizes were calculated from the SEM images of the polished thermally etched surfaces by the linear-intercept method. For dielectric measurement, gold electrodes were

deposited on both faces of the disk samples (5 mm diameter and ~ 1.0 mm thick). The relative permittivity, ϵ was measured by impedance analysis (HP4194A). The transmittance was measured in a spectrophotometer (Miconal-B582), at wavelengths ranging from 200 to 1000 nm for optically polished samples, 600 μm thick. The method used in the electro-optical characterization, determination of the Pockels and Kerr coefficients, is based in the Senarmont configuration illustrated in the **Figure 1** [13]. The birefringence medium (sample) is located between two linear polarizer's, P_1 and P_2 , where the P_2 polarizer is known as analyzer, whit polarizer axis forming angles of $\pm 45^\circ$ in relation to principal axis of the sample, this definite by the electric-field direction applied. Between the sample and the analyzer is located a $\lambda/4$ plate used to compensation the effects caused by the natural birefringence of the medium. Then the analyzer is positioned in the angle β that optimizes the relation between the birefringence and the applied electric-field. In the Equation (1) is presented the relation between birefringence and electric-field for medium with linear and quadratic electro-optic response.

$$\Delta n(E) = -1/2n^3 (rE + RE) \quad (1)$$

where Δn is the birefringence induced for the electric-field E , n is the natural birefringence of the medium, r and R are the Pockels and Kerr electro-optic coefficients, respectively.

3. Results and Discussion

The relative density of PLMN-XPT and PMN-XPT:La at different PT concentration are greater than 96% of the theoretical density as can be seen in **Figure 2**, which is especially suitable for electronic industry application [14]. The relative density of the two system exhibits the tendency to decrease when PT concentration is increased. This can be attributed the loss of PbO (control atmosphere of PbO was not used in this work) [15]. As well can be seen the relative densities of PLMN-XPT ceramics is greater for all PT concentrations when compared with PMN-XPT:La. This possibly associated with the less occupation of La^{3+} in Pb^{2+} sites, implying in the appearance of vacancies in the A and B sites in different quantities [16] (La^{3+} atoms are lighter than Pb^{2+} atoms, and PMN-XPT:La have major number of La atoms).

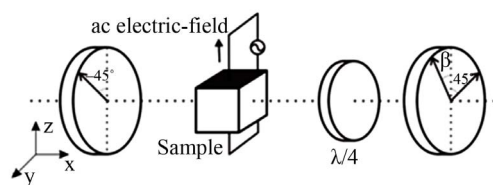


Figure 1. Illustration of the experimental Senarmont method for characterization of the transversal electro-optical effect.

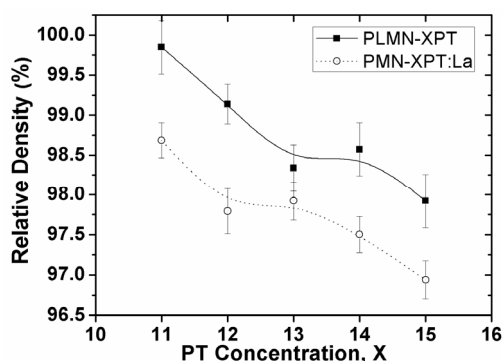


Figure 2. Variation of relative density as a function of PT concentration of the PLMN-XPT and PMN-XPT:La ceramics with $0.11 \leq x \leq 0.15$.

The variation of density is considered as relating to mass loss induced by evaporation of PbO or to variation of temperature of densification relating to the increase of PT, this changes the grain size, porosity could appear which decreases the relative density of ceramics. However the slight decrease of relative density of PLMN-XPT and PMN-XPT:La ceramics can be attributed to the variation of microstructure and to evaporation of lead at elevated sintering temperatures.

The high densification of PLMN-XPT and PMN-XPT:La ceramics is further confirmed by SEM observation, which is shown in Figure 3. All ceramics exhibited similar microstructure as can be seen in the micrograph of polished and thermally attacked surface of PLMN-13PT (shown here).

The variation of grain size with the increase of PT concentration is shown in Figure 4. An increase in PT concentration resulted in a decrease in grain size and a corresponding slight decrease in density [17]. The grain size in PMN-XPT:La is lesser for all concentration when compared to PLMN-XPT because the major quantities of La^{3+} resulted in reduction of grain size as observed by Kim *et al.* in La^{3+} doped PMN-PT ceramics [18].

The XRD patterns of sintered ceramics with different compositions are presented in Figure 5, where a complete perovskite structure (JCPDS 391488) is formed and the pyrochlore or other second phases were not detected.

The permittivity (real, ϵ' and imaginary, ϵ'') was measured at various temperatures in the frequency range 1 kHz - 1MHz. In the Figure 6 can be seen a typical examples of measurements realized in this work. All the samples exhibit typical relaxor behavior [19,20], with the magnitude of ϵ' decreasing with increasing frequency, and the maximum permittivity real, ϵ'_{\max} shifting to higher temperatures, as shown in the PLMN-12PT ceramics (Figure 6). The data of all ceramic analyzed in this work can be seen in the Table 1.

Variations in the shape of ϵ' in function of T curves can be also directly related to the diffuseness coefficient,

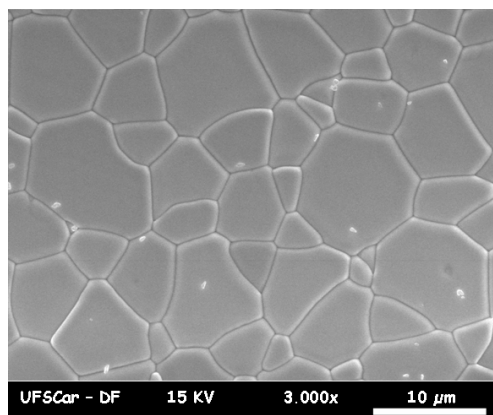


Figure 3. SEM image of surfaces polished and thermally attacked of PLMN-13PT ceramic.

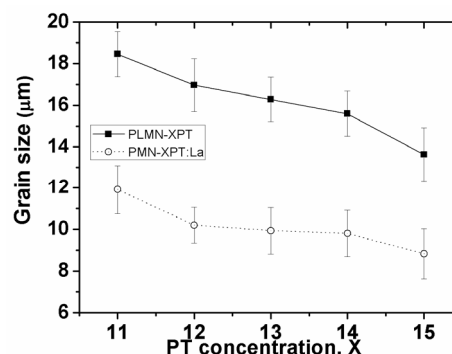


Figure 4. Grain size in function of PT concentration of the PLMN-XPT and PMN-XPT:La ceramics with $0.11 \leq x \leq 0.15$.

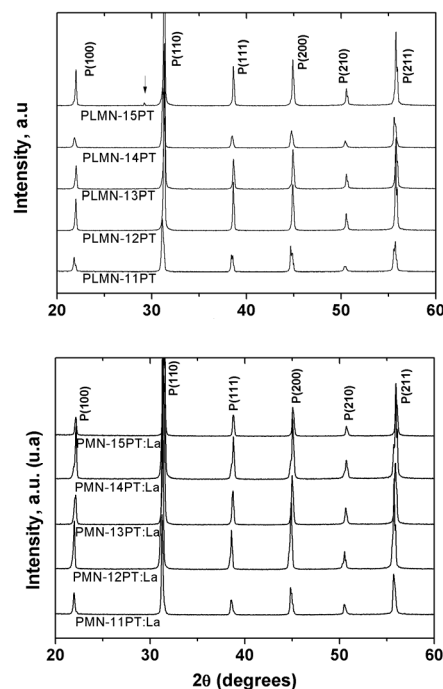


Figure 5. XRD patterns of PLMN-XPT and PMN-XPT:La ceramics with $0.11 \leq x \leq 0.15$.

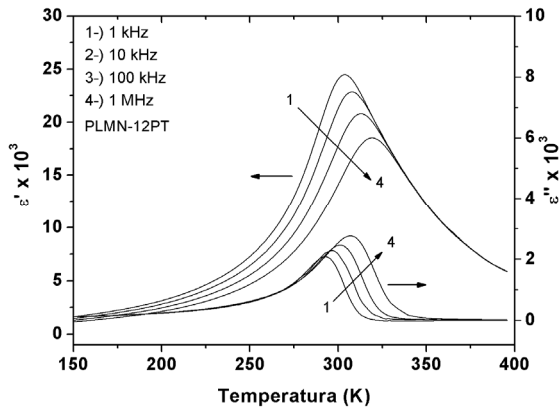


Figure 6. Permittivity real, ϵ' and permittivity imaginary, ϵ'' at various frequencies in function of temperature for PLMN-XPT and PMN-XPT:La ceramics with $0.11 \leq x \leq 0.15$.

Table 1. Dielectric properties of PLMN-XPT and PMN-XPT:La with $0.11 \leq x \leq 0.15$ at 1 kHz.

Ceramic	ϵ'_{\max}	T_{\max} (K)	Δ
PLMN-11PT	27,000	293	1.66
PLMN-12PT	26,800	300	1.65
PLMN-13PT	25,200	305	1.63
PLMN-14PT	29,000	308	1.53
PLMN-15PT	28,000	317	1.55
PMN-11PT:La	25,000	297	1.62
PMN-12PT:La	24,700	299	1.62
PMN-13PT:La	25,100	308	1.62
PMN-14PT:La	23,000	318	1.60
PMN-15PT:La	30,000	319	1.52

δ in **Table 1**, calculated from the Santos Eiras equation [21], which for relaxors reflect the level of disorder in term of the diffusivity of the ϵ'_{\max} . As can be deduced from **Table 1**, the value of ϵ'_{\max} for PMN-XPT:La³⁺ are smaller than PLMN-XPT, inferring that lanthanum additions result in the reduction in ϵ'_{\max} , while increasing the degree of ordering, as observed for Kim *et al.* [18].

The transmission spectrum as a function of wavelength (200 nm - 1100 nm) of PLMN-XPT and PMN-XPT:La ceramics with $0.11 \leq x \leq 0.15$ and 630 μm thickness is presented in **Figure 7**. For both of these stoichiometries formula the percentage of transmitted light begins to rise abruptly at just below 380 nm and then increases only gradually with wavelength about 500 nm. This gradual increase in transmittance continues into the near IR at least through 1100 nm without any noticeable absorption band being observed. This is similar to what was observed for most crystals with oxygen-octahedral perovskites structure [22-24]. From the transmission characterization, we can see that the optical absorption is very small at higher

wavelength range. In general, optical transmission relates to reflection loss and scattering loss. Using the refractive indices measured by Mchenry *et al.* [12], e by the Fresnel expression, the reflection loss of the light at two surfaces was calculated about 20%. Beyond of reflection loss is observed loss by scattering which can be attributed the dispersion by ferroelectrics domain (spontaneous birefringence), increases in the porosity (by loss of PbO) and precipitation of spurious phases. In general the addition of PT increase the transmittance both the PLMN-XPT and PMN-XPT:La, nevertheless exist a concentration optimal of PT in 14%. As previously mentioned the increase of content of PT promotes the densification of the samples, favoring the transmittance, though the sample with PMN-XPT:La present less transmission in comparison with the PLMN-XPT in function of wavelength. This effect is attributed the replacement of lanthanum ions in the sites of the lead, that increased the number of vacancies reducing the density and consequently affecting the transmittance.

In the **Table 2** can be seen the values for the electro-optic Kerr coefficients as a function of PT concentration and stoichiometric formula, which were determined under frequency of 200 Hz, at room temperature. The values of electro-optical coefficients here obtained are similar the reported in literature for La doped PMN-PT ce-

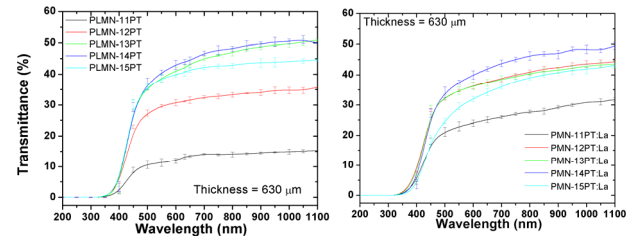


Figure 7. Percent transmission as a function of wavelength for optically polished PLMN-XPT and PMN-XPT:La with $0.11 \leq x \leq 0.15$ and 630 μm thickness.

Table 2. Electro-optical coefficient, R of PLMN-XPT and PMN-XPT:La with $0.11 \leq x \leq 0.15$ calculated under frequency of 200 Hz.

Ceramic	R ($\times 10^{-16}$ m^2/V^2)
PLMN-11PT	8.0
PLMN-12PT	14.1
PLMN-13PT	23.7
PLMN-14PT	10.1
PLMN-15PT	10.3
PMN-11PT:La	7.1
PMN-12PT:La	10.3
PMN-13PT:La	13.0
PMN-14PT:La	9.2
PMN-15PT:La	6.1

amics [12,25] and greater to commercial PLZT ceramics [26]. The Kerr coefficients of the PLMN-XPT ceramics are higher when compared with PMN-XPT:La ceramics because of their major transmittance, since that the phase induced by electro-optical effect is directly proportional intensity of light transmission [27].

4. Conclusion

The ceramics obtained in this study showed high dense and homogeneous microstructure, independent of the stoichiometric which were obtained. The La addition to the PLMN-XPT and PMN-XPT:La relaxor ferroelectric system was found to promote densification and inhibit grain growth, however the PMN-XPT:La ceramic to present smaller density in relation to other composition. The transmittance characterization revealed a transmission of about 50% from 0.45 μm to 1.1 μm , presenting a lower transmission in the samples of PMN-XPT:La. The quadratic electro-optic coefficients, calculated from measurements of birefringence in this work to PMN-XPT and PLMN-XPT ceramics are up to two times higher than the maximum reported for PLZT. Thus confirming the potential use of these system as substitutes for PLZT in electro-optical applications.

5. Acknowledgements

To CAPES, FAPESP and CNPq for the financial support. To Dr. Y. P. Mascarenhas (São Carlos Physics Institute at the University São Paulo), for the use of the XRD laboratory facilities. And to Mr. Francisco José Picon for the technical support.

REFERENCES

- [1] G. A. Smolenskii and A. I. Agranovskaya, "Dielectric Polarization and Losses of Some Complex Compounds," *Soviet Physics—Technical Physics*, Vol. 3, No. 7, 1958, pp. 1380-1382.
- [2] S. L. Swartz and T. R. Shrout, "Fabrication of Perovskite Lead Magnesium Niobate," *Materials Research Bulletin*, Vol. 17, No. 10, 1982, pp. 1245-1250. [doi:10.1016/0025-5408\(82\)90159-3](https://doi.org/10.1016/0025-5408(82)90159-3)
- [3] T. R. Shrout and A. Halliyal, "Preparation of Lead-Based Ferroelectric Relaxors for Capacitors," *The Bulletin of the American Ceramic Society*, Vol. 66, No. 4, 1987, pp. 704-711.
- [4] S. J. Jang, K. Uchino, S. Nomura and L. E. Cross, "Electrostrictive Behavior of Lead Magnesium Niobate Based Ceramic Dielectrics," *Ferroelectrics*, Vol. 27, No. 1, 1980, pp. 31-34. [doi:10.1080/00150198008226059](https://doi.org/10.1080/00150198008226059)
- [5] Y. H. Chen, K. Uchino, M. Shen and D. Viehland, "Substituent Effects on the Mechanical Quality Factor of $\text{Pb}(\text{Mg}_{1/3}\text{Nb}_{2/3})\text{O}_3\text{-PbTiO}_3$ and $\text{Pb}(\text{Sc}_{1/2}\text{Nb}_{1/2})\text{O}_3\text{-PbTiO}_3$ Ceramics," *Journal of Applied Physics*, Vol. 90, No. 3, 2001, pp. 1455-1458. [doi:10.1063/1.1379248](https://doi.org/10.1063/1.1379248)
- [6] L. B. Kong, J. Ma, W. Zhu and O. K. Tan, "Rapid Formation of Lead Magnesium Niobate-Based Ferroelectric Ceramics via a High-Energy Ball Milling Process," *Materials Research Bulletin*, Vol. 37, No. 3, 2002, pp. 459-465. [doi:10.1016/S0025-5408\(01\)00823-6](https://doi.org/10.1016/S0025-5408(01)00823-6)
- [7] E. M. Jayasingh, K. Prabhakaran, R. Sooraj, C. Duragaspad and S. C. Sharma, "Synthesis of Pyrochlore Free PMN-PT Powder by Partial Oxalate Process Route," *Ceramics International*, Vol. 35, No. 2, 2009, pp. 591-596. [doi:10.1016/j.ceramint.2008.01.022](https://doi.org/10.1016/j.ceramint.2008.01.022)
- [8] X. M. Wan, H. Q. Xu, T. H. He, D. Lin and H. S. Luo, "Optical Properties of Tetragonal $\text{Pb}(\text{Mg}_{1/3}\text{Nb}_{2/3})_{0.62}\text{-TiO}_{0.38}$ Single Crystal," *Journal of Applied Physics*, Vol. 93, No. 8, 2003, pp. 4766-4768. [doi:10.1063/1.1561991](https://doi.org/10.1063/1.1561991)
- [9] A. S. Bhalla, R. Guo, A. S. Cross, G. Burns, F. H. Dacol and R. R. Neurgaonkar, "Glassy Polarization in the Ferroelectric Tungsten Bronze $(\text{Ba,Sr})\text{Nb}_2\text{O}_6$," *Journal of Applied Physics*, Vol. 71, No. 11, 1992, pp. 5591-5595. [doi:10.1063/1.350537](https://doi.org/10.1063/1.350537)
- [10] A. S. Bhalla, R. Guo, A. S. Cross, G. Burns, F. H. Dacol and R. R. Neurgaonkar, "Measurements of Strain and the Optical Indices in the Ferroelectric $\text{Ba}_{0.4}\text{Sr}_{0.6}\text{Nbz}$: Polarization Effects," *Physical Review B*, Vol. 36, No. 4, 1987, pp. 2030-2035. [doi:10.1103/PhysRevB.36.2030](https://doi.org/10.1103/PhysRevB.36.2030)
- [11] F. A. Londono, J. A. Eiras and D. Garcia, "New Transparent Ferroelectric Ceramics with High Electro-Optical Coefficients: PLMN-PT," *Cerâmica*, Vol. 57, No. 344, 2011, pp. 404-408.
- [12] D. A. Mchenry, J. Giniewicz, S. J. Jang, A. Bhalla and T. R. Shrout, "Optical Properties of Hot Pressed Relaxor Ferroelectrics," *Ferroelectrics*, Vol. 93, No. 1, 1989, pp. 351-359. [doi:10.1080/00150198908017367](https://doi.org/10.1080/00150198908017367)
- [13] R. Go, "Ferroelectric Properties of Lead Barium Niobate Compositions near the Mosphotropic Phase Boundary," Ph.D. Theses, Pennsylvania State University, Pennsylvania, 1990.
- [14] C. Ding, *et al.*, "Phase Structure and Electrical Properties of $0.8\text{Pb}(\text{Mg}_{1/3}\text{Nb}_{2/3})\text{O}_3$ Relaxor Ferroelectric Ceramics Prepared by the Reaction-Sintering Method," *Physica Status Solidi (A)*, Vol. 207, No. 4, 2010, pp. 979-985. [doi:10.1002/pssa.200925377](https://doi.org/10.1002/pssa.200925377)
- [15] G. S. Snow, "Fabrication of Transparent Electrooptic PLZT Ceramics by Atmosphere Sintering," *Journal of the American Ceramic Society*, Vol. 56, No. 2, 1973, pp. 91-96. [doi:10.1111/j.1151-2916.1973.tb12365.x](https://doi.org/10.1111/j.1151-2916.1973.tb12365.x)
- [16] S. M. Gupta and D. Viehland, "Role of Charge Compensation Mechanism in La-Modified $\text{Pb}(\text{Mg}_{1/3}\text{Nb}_{2/3})\text{O}_3\text{-PbTiO}_3$ Ceramics: Enhanced Ordering and Pyrochlore Formation," *Journal of Applied Physics*, Vol. 80, No. 10, 1996, pp. 5875-5883. [doi:10.1063/1.363581](https://doi.org/10.1063/1.363581)
- [17] N. Kim, D. A. McHenry, S. J. Jang and T. R. Shrout, "Fabrication of Optically Transparent Lanthanum Modified $\text{Pb}(\text{Mg}_{1/3}\text{Nb}_{2/3})\text{O}_3$ Using Hot Isostatic Pressing," *Journal of the American Ceramic Society*, Vol. 73, No. 4, 1990, pp. 923-928. [doi:10.1111/j.1151-2916.1990.tb05137.x](https://doi.org/10.1111/j.1151-2916.1990.tb05137.x)
- [18] N. Kim, W. Huebner, S. J. Jang and T. R. Shrout, "Dielectric and Piezoelectric Properties of Lanthanum-Modified Lead Magnesium Niobium-Lead Titanate Ceram-

- ics,” *Ferroelectrics*, Vol. 93, No. 1, 1989, pp. 341-349.
[doi:10.1080/00150198908017366](https://doi.org/10.1080/00150198908017366)
- [19] L. E. Cross, S. J. Jang, R. E. Newnham, S. Nomura and K. Uchino, “Large Electrostrictive Effects in Relaxor Ferroelectrics,” *Ferroelectrics*, Vol. 23, No. 1, 1980, pp. 187-191. [doi:10.1080/00150198008018801](https://doi.org/10.1080/00150198008018801)
- [20] K. Uchino, S. Nomura, L. E. Cross, S. J. Jang and R. E. Newnham, “Electrostrictive Effect in Lead Magnesium Niobate Single Crystals,” *Journal of Applied Physics*, Vol. 51, No. 2, 1979, pp. 1142-1145. [doi:10.1063/1.327724](https://doi.org/10.1063/1.327724)
- [21] I. A. Santos and J. A. Eiras, “Phenomenological Description of the Diffuse Phase Transition in Ferroelectrics,” *Journal of Physics: Condensed Matter*, Vol. 13, No. 50, 2001, pp. 11733-11740.
[doi:10.1088/0953-8984/13/50/333](https://doi.org/10.1088/0953-8984/13/50/333)
- [22] X. M. Wan, H. S. Luo and X. Y. Zhao, “Refractive Indices and Linear Electro-Optic Properties of $(1-x)\text{Pb}(\text{Mg}_{1/3}\text{Nb}_{2/3})\text{O}_3-x\text{PbTiO}_3$ Single Crystals,” *Applied Physics Letters*, Vol. 85, No. 22, 2004, pp. 5233-5235.
[doi:10.1063/1.1829393](https://doi.org/10.1063/1.1829393)
- [23] C. J. He, L. H. Luo and X. Y. Zhao, “Optical Properties of Tetragonal Ferroelectric Single Crystal Lead Magnesium Niobate Lead Titanate,” *Journal of Applied Physics*, Vol. 100, No. 1, 2006, Article ID: 013112.
[doi:10.1063/1.2217487](https://doi.org/10.1063/1.2217487)
- [24] F. A. Londono, J. Eiras and D. Garcia, “Optical and Electro-Optical Properties of $(\text{Pb},\text{La})\text{TiO}_3$ Transparent Ceramics,” *Optical Materials*, Vol. 34, No. 8, 2012, pp. 1310-1313. [doi:10.1016/j.optmat.2012.02.020](https://doi.org/10.1016/j.optmat.2012.02.020)
- [25] K. Uchino, “Ferroelectric Devices,” Marcel Dekker, New York, 2000.
- [26] K. Uchino, “Electro-Optic Ceramics and Their Display Applications,” *Ceramics International*, Vol. 21, No. 5, 1995, pp. 309-315. [doi:10.1016/0272-8842\(95\)96202-Z](https://doi.org/10.1016/0272-8842(95)96202-Z)
- [27] A. Yariv and P. Yeh, “Optical Waves in Crystals: Propagation and Control of Laser Radiation,” John Wiley & Sons, New York, 1984.